

DYNAMICAL EVOLUTION OF CLUSTERS



M. GIRARDI, M. MEZZETTI, and A. DEVETAK
Dipartimento di Astronomia, Università di Trieste (DAUT)
via Tiepolo 11, I-34100, Trieste, Italy

We consider a sample of about 50 distant galaxy clusters at $z > 0.15$ ($\langle z \rangle \sim 0.3$), each cluster having at least 10 galaxies with available redshift in the literature. We select member galaxies, analyze the velocity dispersion profiles, and evaluate in a homogeneous way cluster velocity dispersions and virial masses. We apply the same procedures already recently applied on a sample of nearby clusters ($z < 0.15$) in order to properly analyze the possible dynamical evolution of galaxy clusters. We do not find any significant difference between nearby and distant clusters. In particular, we consider the galaxy spatial distribution, the shape of the velocity dispersion profile, and the relations between velocity dispersion and X-ray luminosity and temperature. Our results imply little dynamical evolution in the range of redshift spanned by our cluster sample, and suggest that the typical redshift of cluster formation is higher than that of the sample we analyze.

1 Introduction

The knowledge of the properties of galaxy clusters plays an important role in the study of large scale structure formation. In particular, one can use their number density as a function of their mass ("mass function") to constrain cosmological parameters. Several recent works attempt to estimate the value of the matter density parameter Ω_m from the evolution of cluster mass function (e.g., Carlberg *et al.*¹; Borgani *et al.*²).

However, the estimate of cluster masses is not an easy task. Both the virial theorem applied to positions and velocities of cluster member galaxies and the dynamical analysis of hot X-ray emitting gas assume that clusters are systems in dynamical equilibrium, while the mass estimates derived from gravitational lensing phenomena require a good knowledge of cluster geometry.

As for the analysis of the internal dynamics of nearby clusters (at redshift $z \lesssim 0.15$), recent conclusions are based on very large samples (Fadda *et al.*³; Mazure *et al.*⁴; Girardi *et al.*⁵). In particular, Girardi *et al.*⁵ showed that virial masses based on member galaxies are quite consistent with those obtained from X-ray analysis suggesting that most clusters are not very far from dynamical equilibrium.

As for distant clusters, most results come from the analysis of the 16 clusters at intermediate redshifts, $0.18 < z < 0.55$ of CNOC (Canadian Network for Observational Cosmology; Yee *et al.*⁶) which represents a remarkably homogeneous sample. In particular, as found in nearby clusters, Lewis *et al.*⁷ claim for consistency between masses coming from optical and X-ray

data. However, the difficulties of obtaining many redshifts in distant clusters have prevented from building larger samples. Rather, several works, concerning one or a small number of clusters, and using different techniques of analysis, can be found in the literature.

The availability of a variety of techniques, already applied to nearby clusters, suggests their application to distant clusters. We thus ensure the homogeneity of our results over a large range of cosmological distances. A homogeneous analysis is in fact fundamental for the understanding of the evolution of cluster properties. We present the preliminary results of our analysis of a sample of about 50 clusters with $z > 0.15$ where we use the same techniques already used by Girardi *et al.*⁵ (cf. also Fadda *et al.*³) on a sample of 170 nearby clusters (at $z < 0.15$, data from ENACS – ESO Nearby Abell Cluster Survey, Katgert *et al.*⁸ – and other literature).

Unless otherwise stated, we give errors at the 68% confidence level (hereafter c.l.). A Hubble constant of $100 h \text{ km s}^{-1} \text{ Mpc}^{-1}$ and a deceleration parameter of $q_0 = 0.5$ are used throughout.

2 The Data Sample

We analyze a sample of 51 distant galaxy clusters ($z > 0.15$, $< z \leq 0.3$), each cluster having at least 10 galaxies with available redshift in the literature, for a total of ~ 3500 galaxies. The sample is a compilation of published data (cf. Girardi & Mezzetti in preparation for the complete reference list).

In order to select member galaxies, we apply the same procedure as Girardi *et al.*⁵ (cf. also Fadda *et al.*³). First, we use the adaptive kernel technique by Pisani⁹ as described by Girardi *et al.*¹⁰ to find the significant peaks in velocity distributions. Then, we use the combination of position and velocity information to identify possible interlopers in the above-detected systems. We apply the procedure of the “shifting gapper”, i.e. we apply the fixed gap method to a bin shifting along the distance from the cluster center (cf. Fadda *et al.*³).

Finally, we reject galaxies which show strong emission lines. In fact, there are evidences that emission line galaxies enhance the observed velocity dispersion, σ_v , suggesting that these galaxies are not in dynamical equilibrium within the cluster (e.g., Biviano *et al.*¹¹).

We find that 45 cluster fields show only one peak in their velocity distribution, and three fields show two separable peaks, for a total of 51 well separated systems. The other three cluster fields show two strongly superimposed peaks which suggest that their dynamics is strongly uncertain. In the following analyses we consider only the 51 well separated systems. These 51 systems are those used in the comparison with nearby clusters (160 well defined systems, cf. Girardi *et al.*⁵).

3 Internal Dynamics

We estimate the “robust” velocity dispersion line-of-sight, σ_v , by using the biweight and the gapper estimators when the galaxy number is larger and smaller than 15, respectively (cf. RO-STAT routines – see Beers *et al.*¹²), and applying the relativistic correction and the usual correction for velocity errors (Danese *et al.*¹³).

Following Fadda *et al.*³ (cf. also Girardi *et al.*¹⁰) we analyze the “integral” velocity dispersion profile (hereafter VDP), where the dispersion at a given (projected) radius is evaluated by using all the galaxies within that radius, i.e. $\sigma_v(< R)$. The VDP allows to check the robustness of σ_v estimate. In particular, although the presence of velocity anisotropies can strongly influence the value of σ_v computed for the central cluster region, it does not affect the value of the σ_v computed for the whole cluster (e.g., Merritt¹⁴). The VDPs of nearby clusters show strongly increasing or decreasing behaviors in the central cluster regions, but they are flattening out in the external regions (beyond $\sim 1 h^{-1} \text{ Mpc}$, cf. also den Hartog & Katgert¹⁵) suggesting that in such regions they are no longer affected by velocity anisotropies. Thus, while the σ_v -values

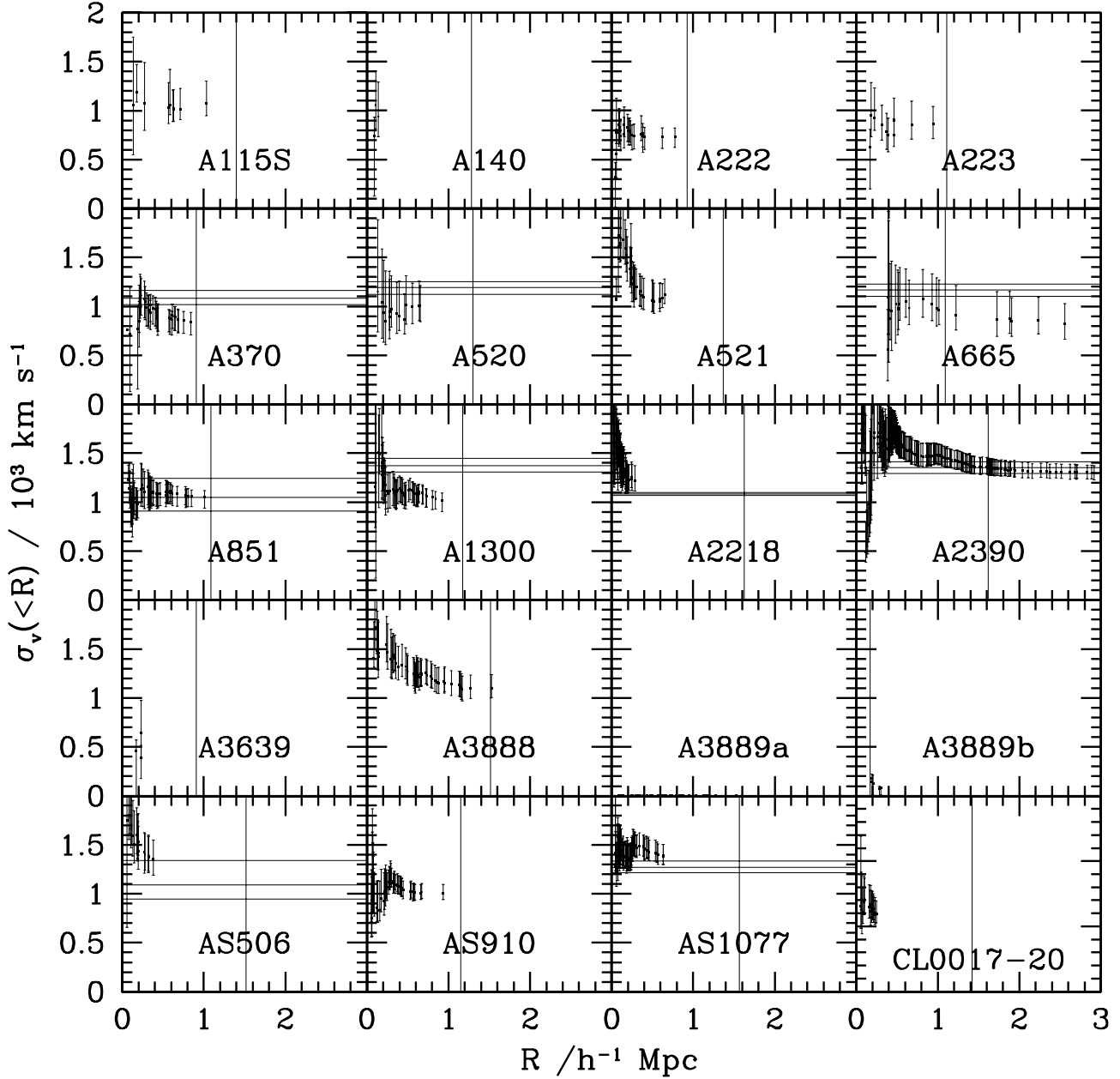


Figure 1: Integrated line-of-sight velocity dispersion profiles $\sigma_v(<R)$, where the dispersion at a given (projected) radius from the cluster center is estimated by considering all galaxies within that radius. The bootstrap error bands at the 68% c.l. are shown. The horizontal lines represent X-ray temperature with the respective errors transformed in σ_v imposing $\beta_{spec} = 1$ (cf. § 4). The vertical faint line indicates the virialized region within R_{vir} .

computed for the central cluster region could be a very poor estimate of the depth of cluster potential wells, one can reasonably adopt the σ_v value computed by taking all the galaxies within the radius at which the VDP becomes roughly constant.

As for the distant clusters we analyze, when the data are good enough, the VDPs show a behavior similar to that of nearby clusters (cf. VDPs for 24 out of 51 clusters in Figure 1). Unfortunately, distant clusters suffer for the poor sampling, and also for the small spatial extension of the sampled cluster region. Indeed, the strongly decreasing VDP in the external sampled regions of some clusters (cf. AS506 in Figure 1) suggests that the correct estimates of velocity dispersions could be smaller than those, σ_v , we can estimate with present data; therefore, in these cases, σ_v should be better interpreted as an upper limit. In other cases, when the member galaxies are too few, the analysis of VDPs does not allow any conclusion.

After fixing the cosmological background, the theory of a spherical model for nonlinear collapse allows to recover the value of the radius of virialization, R_{vir} , within which the cluster can be considered not far from a status of dynamical equilibrium. For nearby clusters Girardi *et al.*⁵ give a first rough estimate of $R_{vir} \sim 0.002 \cdot \sigma_v$ ($km^{-1}s^{-1} h^{-1} Mpc$). A following re-estimate of Girardi *et al.*¹⁶ suggests rather a scaling factor of 0.0017. Since we find that distant clusters have a galaxy distribution similar to that of nearby ones (see in the following), we adopt here the same scaling relation with σ_v : i.e. $R_{vir} \sim 0.0017 \cdot \sigma_v / (1+z)^{3/2}$ ($km^{-1}s^{-1} h^{-1} Mpc$) introducing only the scaling with redshift (cf. also Carlberg *et al.*¹⁷ for a similar relation).

We analyze galaxy distribution in a similar way to that used by Girardi *et al.*⁵, i.e. by fitting the galaxy surface density of each cluster to a King distribution with a variable exponent (hereafter referred to as a “King-like” profile, cf. Girardi *et al.*¹⁸): $\Sigma(R) = \Sigma_0 / (1 + (R/R_c)^2)^\alpha$, where R_c is the core radius and α is the parameter which describes the galaxy distribution in external regions. This surface density profile corresponds to a galaxy volume-density $\rho(r) \propto r^{-(2\alpha+1)}$ for $r \gg R_c$. We perform the fit through the Maximum Likelihood technique, allowing R_c and α to vary from 0.01 to 1 $h^{-1} Mpc$ and from 0.5 to 1.5, respectively. We perform the fit within the circular cluster region, of radius $R_{max,c}$, all contained within the sampled cluster region. We consider only the 30 clusters with at least ten member galaxies within $R_{max,c}$ and we verify our results on a subsample of 13 clusters with $R_{max,c}/R_{vir} > 0.5$.

The median value of α , with the respective errors at the 90% c.l., is $0.63^{+0.08}_{-0.08}$. This value agrees with $\alpha = 0.70^{+0.08}_{-0.03}$ found for nearby clusters, and corresponds to a $\beta_{fit,gal} \sim 0.8$, i.e. to a volume galaxy-density $\rho \propto r^{-2.4}$. After fixing $\alpha = 0.7$, we again fit the galaxy distribution of each cluster, obtaining a median value of $R_c = 0.045^{+0.005}_{-0.015} h^{-1} Mpc$. Thus, in our cluster sample, the typical value of R_c (and $R_{vir}/R_c \sim 20$) is again in agreement with that found in nearby clusters where $R_c = 0.05 \pm 0.01 h^{-1} Mpc$. Hereafter, we assume the above King-modified distribution, with the same parameters of nearby clusters, i.e. $\alpha = 0.7$ and $R_c = 0.05 h^{-1} Mpc$, for all clusters of our sample.

The standard methods used to estimate the cluster mass from member galaxies require that galaxies are in equilibrium within the cluster potential. The cluster mass is then recovered from the knowledge of positions and velocities of the same population of galaxies which are taken as tracers of the cluster potential.

Assuming that clusters are spherical, non rotating systems, and that the internal mass distribution follows galaxy distribution, cluster masses can be computed throughout the virial theorem (e.g., Limber & Mathews¹⁹; The & White²⁰) as:

$$M = M_V - C = \frac{3\pi}{2} \cdot \frac{\sigma_v^2 R_{PV}}{G} - C, \quad (1)$$

where the projected virial radius, $R_{PV} = N(N-1)/(\sum_{i>j} R_{ij}^{-1})$, describes the galaxy distribution and is computed from projected mutual galaxy distances, R_{ij} ; C is the surface term correction to the standard virial mass M_V and it is due to the fact that the system is not entirely enclosed

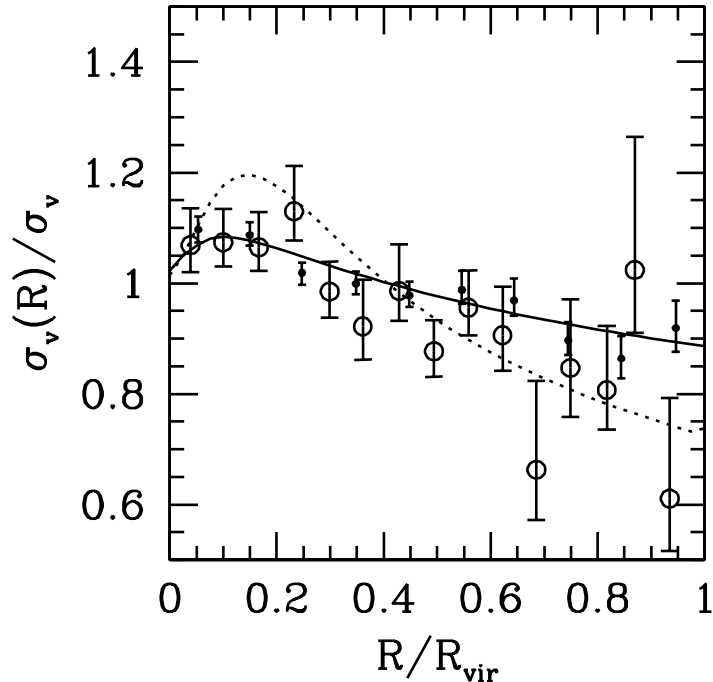


Figure 2: The (normalized) line-of-sight velocity dispersion, $\sigma_v(R)$, as a function of the (normalized) projected distance from the cluster center. The points represent data combined from all clusters and binned in equispacial intervals. We give the robust estimates of velocity dispersion and the respective bootstrap errors. We give the results for distant clusters (open circles) and for nearby clusters taken from Girardi *et al.*⁵ (filled circles). The solid and dotted line represent the models for isotropic and moderate radial orbits of galaxies, respectively.

in the observational sample (cf. also Carlberg *et al.*²¹; Girardi *et al.*⁵).

Following Girardi *et al.*⁵ we want to estimate cluster masses contained within the radius of virialization, R_{vir} . In fact, clusters cannot be assumed in dynamical equilibrium outside R_{vir} and considering small cluster region leads to unreliable measure of the potential (σ_v could be strongly affected by velocity anisotropies) and of the surface term correction (Koranyi & Geller²²).

Unfortunately, only few distant clusters are sampled out to R_{vir} . As for σ_v , the above analysis of the VDP give indications about its reliability, i.e. VDPs which are flat in the external cluster regions will give reliable estimates of σ_v . As for R_{PV} , which describes the galaxy spatial distribution, it can be recovered in an alternative theoretical way from the knowledge of the parameters of the King-like distribution (Girardi *et al.*¹⁸; see also Girardi *et al.*⁵ for a simple analytical approximation in the case of $\alpha = 0.7$ and $R_c/R_{vir} = 0.05$). One can compute R_{PV} at each cluster radius and, in particular, we compute R_{PV} at R_{vir} , which is needed in the computation of the mass within R_{vir} .

The computation of the C correction at the boundary radius, here R_{vir} , is given in eq. 14 of Girardi *et al.*⁵ and requires the knowledge of the velocity anisotropy of galaxy orbits.

Having assumed that in clusters the mass distribution follows the galaxy distribution, one can use the Jeans equation to estimate velocity anisotropies from the data, i.e. from the (differential) profile of the line-of-sight velocity dispersion, $\sigma_v(R)$. We compute the observational $\sigma_v(R)$ by combining together the galaxies of all clusters, i.e. by normalizing distances to R_{vir} and velocities, relative to the mean cluster velocity, to the observed global velocity dispersion σ_v . For nearby clusters the observational profile is well described by a theoretical profile obtained

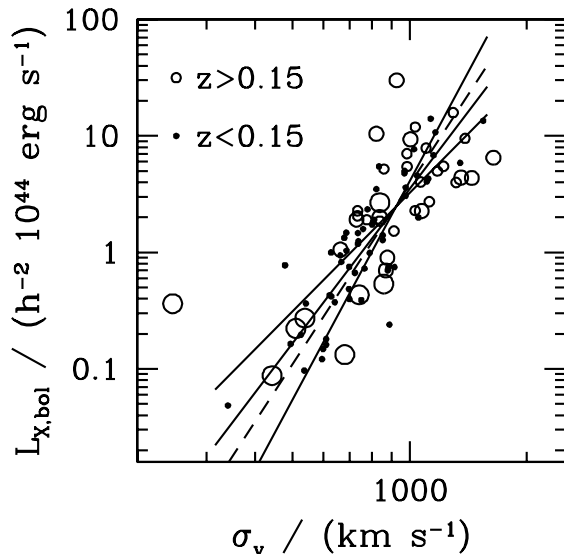


Figure 3: $L_{X,bol}-\sigma_v$ relation for distant (open circles) and nearby clusters (filled circles). For the distant clusters, the circle size decreases with the number of galaxies used to estimate σ_v : the smallest, the intermediate, and the largest circles indicate $N_m \geq 30$, $10 \leq N_m < 30$, and $N_m < 10$, respectively. For the nearby clusters we show results as reported by Borgani *et al.*², all having σ_v estimated at least with 30 galaxy redshifts (Girardi *et al.*⁵) and also belonging to the X-ray Brightest Abell-like Cluster survey (Ebeling *et al.*²⁴). The three solid lines are direct, inverse, and bisecting linear regression for the distant clusters (obtained rejecting the point on the left). The dashed line is the bisecting linear regression for the nearby clusters as computed by Borgani *et al.*².

by the Jeans equation, assuming that velocities are isotropic, i.e. that the tangential and radial components of velocity dispersion are equal (i.e., the velocity anisotropy parameter $\mathcal{A} = 1 - \sigma_\theta^2(r)/\sigma_r^2(r) = 0$). For distant clusters this model is less satisfactory (Figure 2), but cannot be rejected being acceptable at the $\sim 15\%$ c.l. (according to the χ^2 probability).

In order to give C -corrections more appropriate to each individual cluster Girardi *et al.*⁵ used a profile indicator, I_p , which is the ratio between $\sigma_v(< 0.2 \times R_{vir})$, the line-of-sight velocity dispersion computed by considering the galaxies within the central cluster region of radius $R = 0.2 \times R_{vir}$, and the global σ_v . For 33 clusters we can compute the profile indicator and the relative correction; for 18 clusters we cannot define the kind of profile and we assume isotropic orbits (20% of correction).

4 Comparison with X-ray and Lensing Results

We collect X-ray luminosities, in general bolometric ones, $L_{bol,X}$, and temperature, T_X , for 38 and 22 clusters, respectively (most of the data coming from the compilation of Wu *et al.*²³; cf. Girardi & Mezzetti in preparation for the complete reference list).

Figure 3 shows the $L_{X,bol}-\sigma_v$ relation compared to that found by Borgani *et al.*² for nearby clusters. Excluding the leftmost point (J2175.15TR), the resulting bisecting linear regression is

$$\log(L_{bol,X}/10^{44} \text{ erg s}^{-1}) = 4.4_{-1.0}^{+1.8} \log(\sigma_v/\text{km s}^{-1}) - 12.6_{-5.4}^{+3.0}, \quad (2)$$

where errors come from the difference with respect to the direct and the inverse linear regression (Isobe *et al.*²⁵, OLS methods). Our $L_{bol,X}-\sigma_v$ relation is consistent with that of nearby clusters (e.g., White *et al.*²⁶; Borgani *et al.*²; Wu *et al.*²³). As for the point excluded, note that our analysis of J2175.15TR is based only on 19 galaxies, and the estimate of σ_v is recovered from only eight member galaxies (with an error larger than 100%).

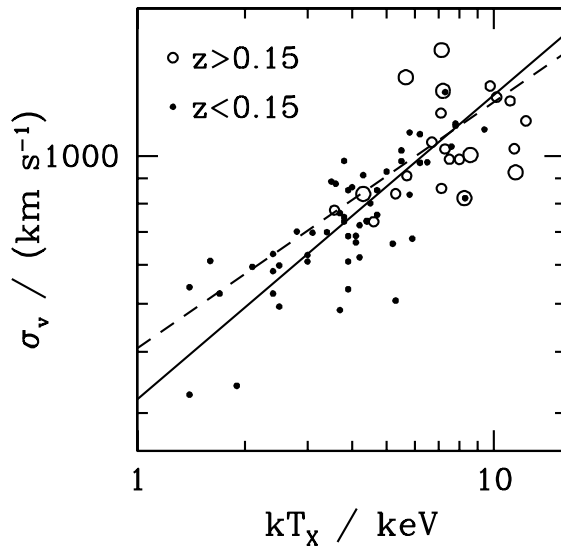


Figure 4: σ_v - T_X relation for distant (open circles) and nearby clusters (filled circles). For the distant clusters, the circle size decreases with the number of galaxies used to estimate σ_v : the smaller and the larger circles indicate $N_m \geq 30$, and $10 \leq N_m < 30$, respectively. For the nearby clusters we show results as reported by Girardi *et al.*⁵, all having σ_v estimated at least with 30 galaxy redshifts, and T_X taken from David *et al.*²⁷ and from White *et al.*²⁶. The solid line is the bisecting linear regression for the nearby clusters as computed by Girardi *et al.*⁵. The dashed line represents the model with the equipartition of energy per unit mass between gas and galaxy components ($\beta_{spec} = 1$).

Figure 4 shows the σ_v - T_X relation compared to that of nearby clusters, as reported by Girardi *et al.*⁵. As for distant clusters, the data have a too small dynamical range to attempt a linear fit: the visual inspection of Figure 4 suggests no difference with nearby clusters in agreement with the result of by Mushotzky & Scharf²⁸ and Wu *et al.*²³. We obtain $\beta_{spec} = \sigma_v^2 / (kT / \mu m_p) = 0.88_{-0.17}^{+0.14}$, where $\mu = 0.58$ is the mean molecular weight and m_p the proton mass (median value with errors at the 90% c.l.). This value of β_{spec} is in good agreement with the value of $\beta_{spec} = 0.88 \pm 0.04$ for nearby clusters (cf. Girardi *et al.*⁵). Moreover, we find no correlation between β_{spec} and redshift (cf. also Wu *et al.*²³).

Under the assumption that the hot diffuse gas is in hydrostatic and isothermal equilibrium with the underlying gravitational potentials of clusters, one can obtain the X-ray cluster masses provided that the gas temperature and radial profile of gas distribution are known. The availability of T_X allow us to compute the mass within R_{vir} for 22 clusters according to $M_X = (3\beta_{fit,gas} kT \cdot R_{vir}) / (G\mu m_p) \cdot (R_{vir}/R_x)^2 / [1 + (R_{vir}/R_x)^2]$, where we adopt the gas distribution given by the β -model with typical parameters (slope $\beta_{fit,gas} = 2/3$ and core radius $R_x = 0.125 h^{-1} Mpc$, e.g., Jones & Forman²⁹). We find mass values consistent with our optical virial estimates, i.e. $M/M_X = 1.02$ (0.86–1.32) for the median value and the range at the 90% c.l..

As for gravitational lensing masses, we resort to estimates found in the literature. We collect projected estimates from weak gravitational lensing analysis, M_L , for 18 clusters (cf. Girardi & Mezzetti in preparation for the complete reference list). In order to compare our optical virial masses to M_L , we project and rescale our masses M within the corresponding radius using the fitted galaxy spatial distribution. We obtain $M_{opt,L}/M_L = 1.30$ (0.63–2.13) (median value and range at the 90% c.l.). Moreover, we do not find any correlation between M/M_X or $M_{opt,L}/M_L$ and redshift.

Our finding are in agreement with other recent studies which find, on average, no evidence

of discrepancy between different mass estimates as computed within large radii, thus suggesting that distant clusters are not far from global dynamical equilibrium (e.g., Allen³⁰; Lewis *et al.*⁷). Note that we avoid to consider mass determination in very central cluster regions since our analysis of cluster members give poor constrains on mass distribution on these scales. Indeed, the assumption of dynamical equilibrium seem to break down in the very central regions as suggested by comparisons with strong lensing mass estimates (e.g., Allen³⁰; Lewis *et al.*⁷).

5 Summary and Conclusions

In order to properly analyze the possible dynamical evolution of galaxy clusters we apply the same procedures already applied on a sample of nearby clusters (170 clusters at $z < 0.15$ from ENACS and other literature, Girardi *et al.*⁵, cf. also Fadda *et al.*³) to a corresponding sample of distant clusters.

We consider a sample of 51 distant galaxy clusters at $z > 0.15$ ($< z > \sim 0.3$), each cluster having at least 10 galaxies with available redshift in the literature. A part from three cluster field showing two overlapping peaks in their velocity distribution and so large uncertainties in their dynamics, 45 fields show only one peak in their velocity distribution and three fields show two separable peaks for a total of 51 well defined cluster systems. These 51 systems are those used in the comparison with nearby clusters (160 well defined systems).

We select member galaxies, analyze the velocity dispersion profiles, and evaluate in a homogeneous way cluster velocity dispersions and virial masses.

As a main general result, we do not find any significant evidence for dynamical evolution of galaxy clusters. More in detail, our results can be summarized as follows.

- The galaxy spatial distribution is similar to that of nearby clusters, i.e. the fit to a King-like profile gives a two-dimensional slope of $\alpha = 0.7$ and a very small core radius of $R_c = 0.05 h^{-1} Mpc$.
- When data are good enough, the integrated velocity dispersion profiles of distant clusters show a behavior similar to those of nearby clusters, i.e. they show strongly increasing or decreasing behaviors in the central cluster regions, but are flattening out in the external regions suggesting that in such regions, they are no longer affected by velocity anisotropies.
- The average velocity dispersion profile can be explained by a model with isotropic orbits, which well describe also nearby clusters. Possible evidences for more radial orbits are not statistically significant.
- There is no evidence of evolution in both $L_{bol,X}-\sigma_v$ and σ_v-T_X relations, thus in agreement with previous results (Mushotzky & Scharf²⁸; Borgani *et al.*²).

Moreover, on average, within the large scatter of present data, we find no significant evidence of discrepancies between our virial mass estimates and those from X-ray and gravitational lensing data, thus suggesting that distant clusters are not far from global dynamical equilibrium (cf. also Allen³⁰; Lewis *et al.*⁷).

We conclude that the typical redshift of cluster formation is higher than that of our sample in agreement with previous suggestions (e.g., Schindler³¹; Mushotzky³²). In particular, we agree with preliminary results by Adami *et al.*³³, who applied the same techniques used for the nearby ENACS clusters on 15 distant clusters, ($< z > \sim 0.4$) from the Palomar Distant Cluster Survey (Postman *et al.*³⁴).

Although some clusters at very high redshift, e.g. $z > 0.8$, are already known (e.g., Gioia *et al.*³⁵; Rosati *et al.*³⁶), the construction of a large cluster sample useful for studying internal dynamics will require a strong observational effort. We stress how both the poor number of

galaxies and the small spatial extension of some clusters can affect the robustness of their resulting properties.

References

1. R.G. Carlberg *et al.*, *Apj* **476**, L7 (1997)
2. S. Borgani *et al.*, *Apj* **527**, 561 (1999)
3. D. Fadda *et al.*, *Apj* **473**, 670 (1996)
4. A. Mazure *et al.*, *A&A* **310**, 31 (1996)
5. M. Girardi *et al.*, *Apj* **505**, 74 (1998)
6. H.K.C. Yee *et al.*, *ApjS* **102**, 269 (1996)
7. A.D. Lewis *et al.*, *Apj* **517**, 587 (1999)
8. P. Katgert *et al.*, *A&AS* **129**, 399 (1998)
9. A. Pisani, *MNRAS* **265**, 706 (1993)
10. M. Girardi *et al.*, *Apj* **457**, 61 (1996)
11. A. Biviano *et al.*, *A&A* **321**, 84 (1997)
12. T.C. Beers *et al.*, *AJ* **100**, 32 (1990)
13. L. Danese *et al.*, *A&A* **82**, 322 (1980)
14. D. Merritt, *ASP Conf. Ser.* **5**, 175 (1988)
15. R. den Hartog and P. Katgert, *MNRAS* **279**, 349 (1996)
16. M. Girardi *et al.*, *Apj* **506**, 45 (1998)
17. R.G. Carlberg *et al.*, *Apj* **478**, 462 (1997)
18. M. Girardi *et al.*, *Apj* **438**, 527 (1995)
19. D.N. Limber and W.G. Mathews *et al.*, *Apj* **132**, 286 (1960)
20. L.S. The and S.D.M. White, *AJ* **92**, 1248 (1960)
21. R.G. Carlberg *et al.*, *Apj* **462**, 32 (1996)
22. D.M. Koranyi and M.J. Geller, *AJ* **119**, 44 (2000)
23. X.P. Wu *et al.*, *Apj* **524**, 22 (1999)
24. H. Ebeling, *MNRAS* **281**, 799 (1996)
25. T. Isobe *et al.*, *Apj* **364**, 104 (1990)
26. D.A. White *et al.*, *MNRAS* **292**, 419 (1997)
27. L. P. David *et al.*, *Apj* **412**, 479 (1993)
28. R.F. Mushotzky and C.A. Scharf, *Apj* **482**, L13 (1997)
29. C. Jones and W. Forman, in *Clusters and Superclusters of Galaxies*, ed. A. C. Fabian (Dordrecht: Kluwer), p. 49 (1992)
30. S.W. Allen, *MNRAS* **296**, 392 (1998)
31. S. Schindler, *A&A* **349**, 435 (1999)
32. R.F. Mushotzky, *ASP Conf. Ser.* **193**, 323 (2000)
33. C. Adami *et al.*, in *proc. of the 1999 IGRAP Conference*, preprint astro-ph/9907366 (1999)
34. M. Postman *et al.*, *AJ* **111**, 615 (1996)
35. I.M. Gioia *et al.*, *AJ* **117**, 2608 (1999)
36. P. Rosati *et al.*, *AJ* **118**, 76 (1999)